The FLUKA cross sections for galactic cosmic-ray propagation studies

Mario Nicola Mazziotta[a,*] and Pedro De la Torre Luque[b]

[a]*Istituto Nazionale di Fisica Nucleare, Sezione di Bari, via Orabona 4, I-70126 Bari, Italy*

[b]*Stockholm University and The Oskar Klein Centre for Cosmoparticle Physics, Alba Nova, 10691 Stockholm, Sweden*

E-mail: Marionicola.Mazziotta@ba.infn.it, pedro.delatorreluque@fysik.su.se

Current measurements of cosmic-ray fluxes have reached unprecedented accuracy thanks to the new generation of experiments, and in particular the AMS-02 mission. At the same time, significant progress has been made in the propagation models of galactic cosmic rays. These models include several propagation parameters, which are usually inferred from the ratios of secondary to primary cosmic rays, and which depend on the cross sections describing the collisions among the various species of cosmic-ray nuclei with the interstellar medium (spallation cross sections). The current spallation cross sections are based on set of parameterizations mixing (few) data points and simulation predictions for those channels with no measurements. In this work, we present new sets of spallation cross sections of cosmic-ray interactions in the Galaxy, both inelastic and inclusive, computed with FLUKA simulation code that has been extensively tested against data. Furthermore, these cross sections have been implemented in the DRAGON2 code to characterize the spectra of CR nuclei up to Z=26 (Iron) and study the main propagation parameters predicted from the spectra of secondary CRs such as B, Be and Li. We discuss these results and their implications.

27th European Cosmic Ray Symposium (ECRS 2022)
25-29 July 2022
Nijmegen, the Netherlands

---

*Speaker

1. Introduction

Galactic cosmic rays (CRs), injected and accelerated in astrophysical sources, propagate throughout the Galaxy for millions of years, occasionally interacting with the gas in the interstellar medium (ISM) through spallation reactions that produce secondary particles, such as gamma rays, neutrinos or secondary nuclei that we call secondary CRs. The amount of secondary CRs provides direct information about the mean grammage traversed by primary CRs (i.e. the amount of gas per unit area that primary CRs cross during their journey) and, consequently, about the time that these CRs reside in the Galaxy. Measuring the spectra of secondary CRs such as Li, B, Be or F provides further information on how CRs interact with the magneto-hydrodynamical (MHD) turbulence in the ISM plasma and the energy dependence of these interactions.

The transport of CRs in the Galaxy is conventionally studied as a diffusive process characterised by a diffusion coefficient which is, basically, a power-law in energy ($D \propto E^{\delta}$), whose spectral index δ is intimately related to the MHD interactions that CRs undergo. The secondary-to-primary flux ratios, such as the B/C ratio, are used to determine the diffusion coefficient; in fact, the two quantities are strictly related, as can be seen from the approximate relation $N_{sec}(E)/N_{prim}(E) \propto \sigma(E)/D(E)$, where $\sigma(E)$ is the spallation cross section of production of the secondary CR involved. Therefore, a precise evaluation of these ratios is crucial nowadays to unveil the process of transport of charged particles in the Galaxy and its main features, which also requires a good knowledge of cross sections of CR interactions in a broad energy range.

While current CR data are extremely precise since the past decade, recent studies have proved the need of improving the knowledge of the spallation cross sections to reduce the uncertainty related to the determination of the diffusion coefficient from the secondary-to-primary flux ratios [1–3]. Spallation cross sections in the GeV-TeV energy range are in fact measured with very poor accuracy (20%), and often no data are available at all for the energies of interest. In addition, since the nuclear models describing these kind of interactions are mainly adjusted to reproduce accelerator data, the cross sections computed from these models are not totally consistent with the available data in the GeV-TeV range. Hence, simulations usually rely on parameterizations fitted to the very scarce, limited and uncertain experimental data.

Nevertheless, these Monte Carlo simulation codes experienced a positive boost in the last years, usually driven by radiological and medical applications, which need to accurately describe the transport of ions in different materials and their interactions. The FLUKA Monte Carlo nuclear code [1] has been optimized to be used in different kinds of astrophysical studies, with special attention to CR interactions [4–7]. The FLUKA code can be used to transport particles in arbitrarily complex geometries and magnetic fields and study their nuclear interactions with hadrons and nuclei from the MeV/n up to 10 PeV.

Here we give an overview of the main results presented in Ref. [8], where the full cross-section network for CR interactions up to iron nuclei (Z=26) was computed using FLUKA. These cross sections are tested against data and have been implemented in a customized version [2] of the DRAGON2 transport code [9, 10] to study the different ratios of the secondary CRs B, Be and

---

[1]http://www.fluka.org/fluka.php

[2]A similar version of this code can be downloaded at https://doi.org/10.5281/zenodo.4461732

Li and the propagation parameters derived from these predictions through a Markov chain Monte Carlo (MCMC) analysis [11] of the most recent data from the AMS-02 collaboration [12].

In this work, inelastic and inclusive cross sections of all stable isotopes, from protons to iron impinging on helium and hydrogen as targets (representing the main composition of the ISM gas) have been calculated with FLUKA from 1 MeV/n to 35 TeV/n, using 176 bins equally spaced in a logarithmic scale.

2. FLUKA cross sections

Inelastic cross sections σ_{inel} are related to the probability of destruction of a nucleus when it interacts with another particle; their effects on the calculation of the CR spectrum become significant only at low energies, when the time-scale of inelastic collisions ($\tau_{inel}^{-1} \sim v\, n_{ISM} \sigma_{inel}(E)$, where v is the speed of the particle and n_{ISM} is the target number density) is smaller than the diffusion time-scale ($\tau \sim H^2/2D(E)$, where H is Galactic halo size and $D(E)$ is the diffusion coefficient). Experimental data on inelastic cross sections with a proton target are measured with a precision $\leq 15\%$ in the GeV range. The inelastic cross sections computed with FLUKA show a good agreement with data and with other dedicated parameterizations, consistent in the whole energy range studied within $\sim 25\%$ discrepancies. For interactions of nuclei heavier than Ne (Z=10) with protons, for which experimental data in the GeV range is mainly absent, the cross sections predicted from FLUKA differ from those predicted from dedicated parameterizations by $\sim 20\%$, and differnces are Meanwhile, a confirmation that we are correct can be seen in your Fig.5 (p.6)roughly independent of energy [8].

In turn, inclusive cross sections regulate the rate of production of secondary CRs ($\tau_{p \to s}^{-1} \sim v_p n_{ISM} \sigma_{p \to s}(E)$, where v_p is the speed of the projectile nucleus, p, and $\sigma_{p \to s}$ is the cross section of production of the secondary particle, s, from the interaction of the projectile particle with the target nucleus). These are sometimes poorly known because of the experimental difficulties to perform the measurements, and the uncertainties associated to inclusive cross-section data are of $\sim 20\% - 30\%$ in the GeV range. In addition, inclusive cross sections should also include the decay of ghost nuclei (i.e. short-lived nuclei generated in spallation reactions, which have a negligible lifetime compared to typical CR propagation times, and decay into the secondary nucleus that we are considering) in the current CR propagation codes. The inclusive cross sections including this effect are referred to as cumulative inclusive cross sections.

Figure 1 shows the total (i.e. cross sections of interactions with a gas with the ISM composition) cumulative cross sections of production of some isotopes of B, Be and Li from C and O (the main contributors to the production of these secondary CRs). Here we compare the computed FLUKA cross sections with well-known dedicated cross section parameterizations, commonly used in CR transport codes, i.e. the GALPROP [13] and DRAGON2 [1] parameterizations and the cross sections calculated with the WNEW03 [14] and YIELDX [15] (TS98 in the legend) codes.

As we see, the FLUKA cross sections are very consistent with the predictions from the other parameterizations, which is remarkable since our predictions completely rely on theory-based interaction models and not on fits to cross section data. We highlight that both the normalization and energy dependence of these cross sections is compatible with the most updated parameterizations in the whole energy range. In addition, the position of the predicted resonances are also in good
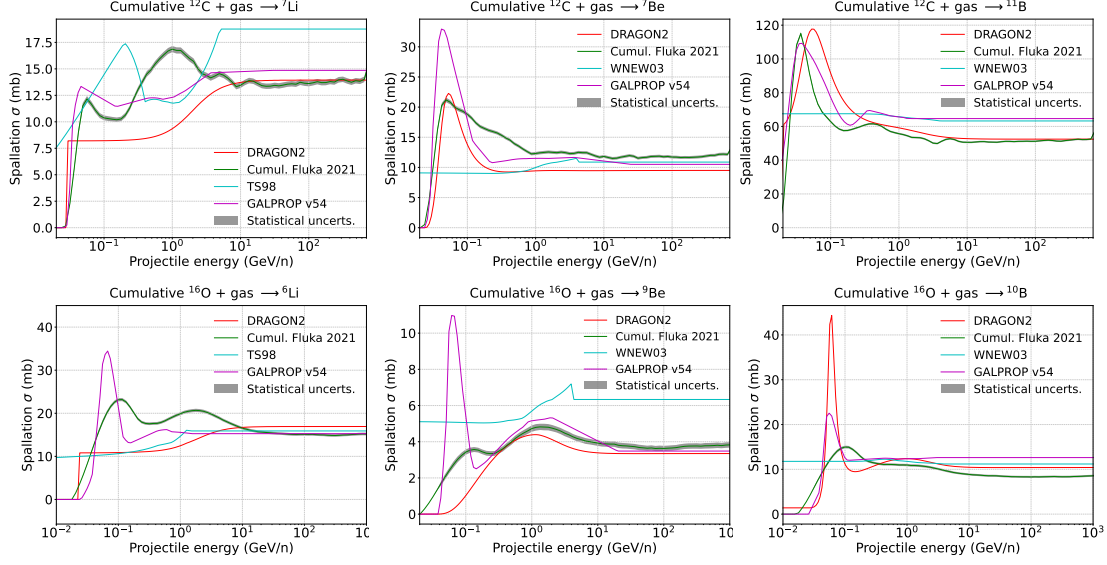
Figure 1: Spallation cross sections of CRs interaction with ISM gas computed with FLUKA compared to the most widely used parameterisations, for the production of isotopes of B, Be and Li from ^{12}C and ^{16}O as projectiles.

agreement with those parameterized from data. We observe that such good consistency is found in most channels of production of isotopes of B, Be and Li from interactions of C, N, O, Ne, Mg and Si with gas, which are the main primary CR species producing these secondaries. We remark the importance of having reliable cross section predictions for those channels in which experimental data is totally absent (meaning that the parameterizations are merely extrapolations in these channels), as happens for the channels of production of heavy secondary CRs, like ^{26}Al for example.

3. CR transport predictions using the FLUKA cross sections

To study the spectra of B, Be and Li derived with the FLUKA cross sections and the propagation parameters inferred from their ratios, we have implemented these cross sections in the DRAGON2 code. The same injection and propagation set-up as presented our previous works [1, 8, 11] is used, which includes reacceleration and neglects convection. Solar modulation is treated with the force-field approximation [16]. In this work, we focus on the results obtained with the diffusion coefficient parameterized as:

$$D = D_0 \beta^\eta \frac{(R/R_0)^\delta}{\left[1 + (R/R_b)^{\Delta\delta/s}\right]^s} \ , \tag{1}$$

Here β is the speed of particle in units of the speed of light, $R_0 = 4$ GV is the rigidity at which the diffusion coefficient is normalized, $\Delta\delta = 0.14$, $R_b = 312$ GV and $s = 0.04$ [11]. The the free parameters entering the fit are the normalization D_0 and the exponent η. The use of the diffusion coefficient of Eq. 1 requires using as injection spectrum a broken power-law with a break set at 8 GeV.

B/C best-fit parameters	FLUKA	GALPROP	DRAGON2
D_0/H (10^{28} cm^2 s^{-1} kpc^{-1})	0.82 ± 0.03	0.94 ± 0.04	0.97 ± 0.04
v_A (km/s)	23.3 ± 2.3	$24.4 \pm 3.$	$22. \pm 3.6$
η	-0.67 ± 0.13	-0.66 ± 0.12	-0.78 ± 0.13
δ	0.45 ± 0.01	0.45 ± 0.01	0.44 ± 0.01

Table 1: Propagation parameteres found in the MCMC analysis of the B/C flux ratio. The halo size value, H, obtained from the ^{10}Be flux ratios is 7.54 kpc. The errors shown here correspond only to statistical uncertainties.

The starting point of this analysis is to find the propagation parameters that allow us to reproduce the boron-over-carbon (B/C) spectrum reported by AMS-02. The injection spectra of nuclei up to iron are adjusted recursively, along with the propagation parameters, to reproduce the AMS-02 data [12]. This analysis yields the values of the propagation parameters entering in the fit which are reported in Table 1. This table also reports those parameters found for the same analysis performed using the DRAGON2 and GALPROP parameterizations. As we can see, the parameters obtained using the FLUKA cross sections are consistent within 1σ with those obtained using dedicated parameterizations, except for the normalization of the diffusion coefficient. This is something remarkable and achieved for the first time with a set of cross sections derived from fundamental models of nuclear interactions.
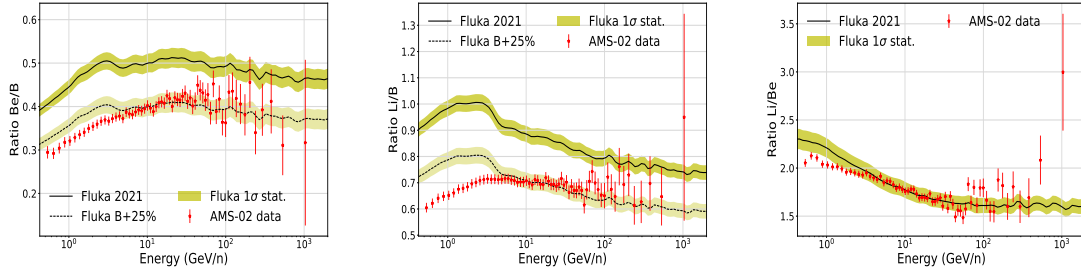

Figure 2: Be/B, Li/B and Li/Be ratios obtained with the FLUKA computations, together with the band of statistical uncertainties due to the spallation cross sections calculation.

One of the most important tools for the study of the cross sections used to evaluate the spectra of secondary CRs are the flux ratios among them (Be/B, Li/B and Li/Be), which are shown in Fig. 2. At high energy, these ratios mainly depend on the ratio of the cross sections of the CR species involved and on the injection spectra of primary CRs, which are adjusted to reproduce the AMS-02 data. In this figure, we show a band of statistical uncertainty associated to the uncertainty related to the determination of the FLUKA cross sections. As can be seen in the figure, while the Li/Be ratio reproduces within 1σ uncertainty the AMS-02 data above ~ 2 GeV, the ratios involving B are overestimated of a roughly constant $20-25\%$ above 3 GeV. We remark that this discrepancy is yet within the typical uncertainty on cross sections measurements above the GeV. However, this discrepancy means that, as happens with the parameterizations commonly used in CR studies, they are not able to reproduce simultaneously B, Be and Li fluxes. A simultaneous solution to this

discrepancy and to the discrepancy found in the value of D_0 with respect to the parameterizations would be to renormalize the cross sections of B production by about a 20%. The result of applying this scaling to the B production cross sections is shown in the figure as a dashed line and leads to a good simultaneous reproduction of the AMS-02 spectra of B, Be and Li above ~ 3 GeV.

To evaluate the size of the halo we analyse the ratios of ^{10}Be to ^{9}Be and to the total flux of Be. Full details can be found in ref. [8]. This fit yields a value of the halo size of $\sim (7.5^{+1.13}_{-0.95})$ kpc, similar to estimations with other cross sections ($H \sim (6.76 \pm 1)$ kpc for the DRAGON2 cross sections and $H \sim (6.93 \pm 0.98)$ kpc for the GALPROP ones).
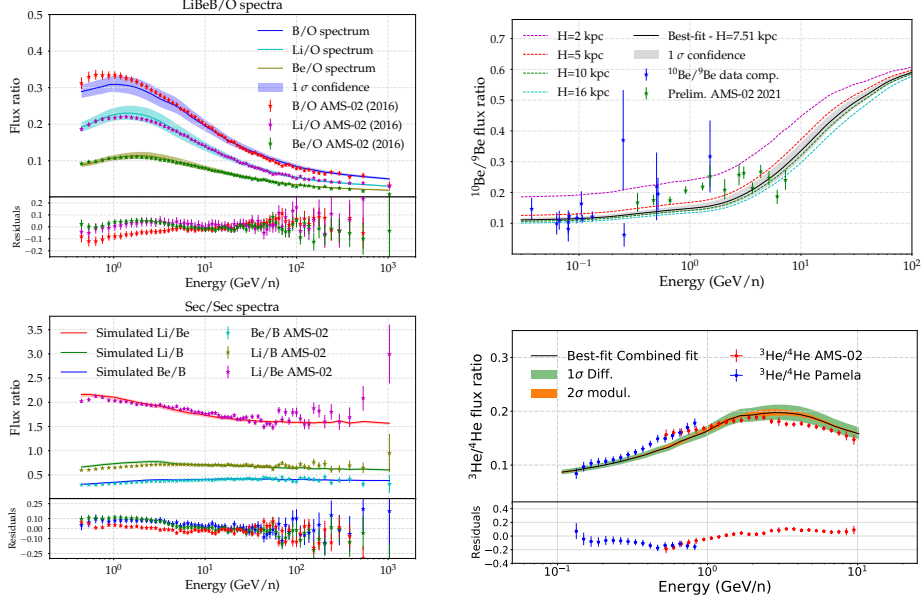

Figure 3: Top-left panel: Secondary-over-secondary flux ratios of B, Be and Li computed using the propagation parameters and cross sections scaling factors found in the combined analysis, compared to the AMS-02 experimental data. **Lower-left panel:** B/O, Be/O and Li/O flux ratios predicted with the parameters determined by the MCMC combined analysis for the DRAGON2 cross sections. **Top-right panel:** ^{10}Be/^{9}Be flux ratio compared to available experimental data. **Lower-right panel:** Predicted ^{3}He/^{4}He flux ratio compared to Pamela and AMS-02 data. Residuals, calculated as model-data/model are also shown. This ratio is calculated with the diffusion coefficient obtained from the combined fit.

3.1 Combined analysis of B, Be and Li

The final test in the study of the spectra of secondary CRs evaluated with the FLUKA cross sections is a combined analysis including the ratios of B, Be and Li to C and O (B/C, B/O, Be/C, Be/O, Li/C and Li/O) and the respective secondary-to-secondary flux ratios (Be/B, Li/B, Li/Be) with a Markov Chain Monte Carlo (MCMC) algorithm presented in a previous work [11]. This analysis includes scaling factors as nuisance parameters, that renormalise the cross sections of production of B, Be and Li and, associated to these scaling factors, a penalty factor that penalises large variations of the original cross sections. The result of this analysis is a set of propagation parameters and scaling factors that are able to simultaneously reproduce all the ratios of B, Be and Li within the 1σ statistical uncertainties in the determination of the propagation parameters. This

is shown in Figure 3, where we report the ratios of Be/B, Li/B and Li/Be, B/O, Be/O, Li/O and the ^{10}Be/^{9}Be ratio included in the fit. We highlight that the diffusion coefficient obtained from these combined analyses allows us to reproduce, at the same time, the ^{3}He/^{4}He flux ratio, shown in the lower-right panel, which is evidence that the diffusion coefficient predicted from the light secondary CRs is compatible for the different nuclei within uncertainties.

These analyses predict a spectral index of the diffusion coefficient ~ 0.36, which is compatible with the value found in Ref. [11]. This value is also consistent with the basic predictions from wave-particle interactions, for which the standard spectrum of plasma waves leads to a spectral index of the diffusion coefficient which is $0.33 \lesssim \delta \lesssim 0.5$. Finally, another crucial point of this analysis are the cross-section scaling factors. These are 1.18, 0.94 and 0.93 for B, Be and Li, respectively, with 1σ statistical uncertainties of $\sim \pm 0.01$. However, we highlight that there are other systematic uncertainties related to the determination of these scale factors, like those related to the gas distribution used, and could make the total systematic uncertainties in the determination of these scale factors larger than 5% [11].

Finally, we used the Local Interstellar spectrum (LIS) predicted from the combined analysis described above to study the diffuse gamma-ray emission. In particular, we tested the local HI gamma-ray emissivity spectrum using Fermi-LAT gamma-ray data [17]. The dominant contribution to this observable at high energies is the gamma-ray emission originating from the decay of unstable particles formed via nuclear reactions (hadronic emission), such as pions. As shown in Figure 4, the hadronic emission allows us to reproduce the Fermi-LAT emissivity within 1σ statistical uncertainties, assuming an ISM composition with relative abundance of H : He : C : N : O : Ne : Mg : Si = 1 : 0.096 : 4.65 \times 10^{-4} : 8.3 \times 10^{-5} : 8.3 \times 10^{-4} : 1.3 \times 10^{-4} : 3.9 \times 10^{-5} : 3.69 \times 10^{-5}$.
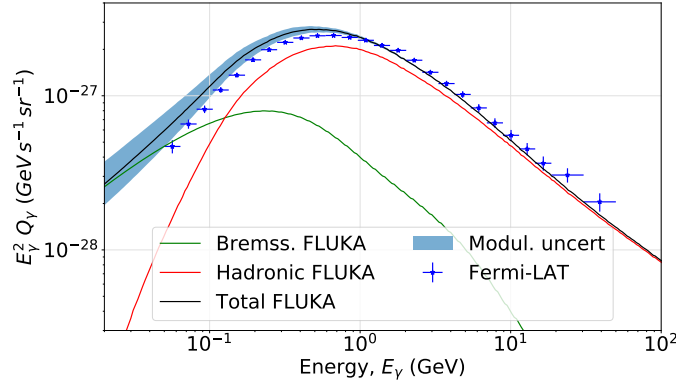

Figure 4: Local HI gamma-ray emissivity spectrum for the propagation parameters derived from the combined analysis. An uncertainty band related to solar modulation uncertainty is also shown.

4. Conclusions

In this work, we presented the FLUKA cross sections for Galactic CR propagation studies as an alternative and an improvement with respect to dedicated cross sections parameterizations. We have tested the spectra of B, Be and Li and evaluated the main propagation parameters inferred

from AMS-02 data, demonstrating that every CR observable can be reproduced with accuracy and at the level of precision of current CR parameterizations.

We showed that the FLUKA cross sections allow us to reproduce simultaneously the light secondary CRs B, Be, Li and ^{3}He when introducing nuisance scaling factors to renormalize the overall cross sections of production of B, Be and Li. The scaling factors obtained are of ~ 1.18, ~ 0.94 and ~ 0.93 for B, Be and Li respectively, which are below the typical average experimental uncertainties of cross sections measurements for the best known channels.

Finally, from the study of the diffuse gamma-ray emission, we have determined the need of including a break in the injection spectrum of electrons at a few GeV, inferred from the local HI gamma-ray emissivity and the diffuse IC emission at MeV energies.

References

[1] P. De la Torre Luque *et al.*, JCAP **03**, 099 (2021), arXiv:2101.01547 [astro-ph.HE] .

[2] N. Weinrich *et al.*, The Astrophysical Journal **639**, A131 (2020), arXiv:2002.11406 [astro-ph.HE] .

[3] M. Korsmeier and A. Cuoco, Phys. Rev. D **103**, 103016 (2021), arXiv:2103.09824 [astro-ph.HE] .

[4] G. Battistoni *et al.*, Annals of Nuclear Energy **82**, 10 (2015).

[5] M. N. Mazziotta *et al.*, Phys. Rev. D **101**, 083011 (2020), arXiv:2001.09933 [astro-ph.HE] .

[6] M. N. Mazziotta *et al.*, AstroPart. Phys. **81**, 21 (2016), arXiv:1510.04623 [astro-ph.HE] .

[7] M. Ackermann *et al.* (Fermi-LAT), Phys. Rev. D **93**, 082001 (2016), arXiv:1604.03349 [astro-ph.HE] .

[8] P. De la Torre Luque, M. N. Mazziotta, A. Ferrari, F. Loparco, P. Sala, and D. Serini, JCAP **07**, 008 (2022), arXiv:2202.03559 [astro-ph.HE] .

[9] C. Evoli *et al.*, JCAP **02**, 015 (2017), arXiv:1607.07886 [astro-ph.HE] .

[10] C. Evoli *et al.*, JCAP **07**, 006 (2018), arXiv:1711.09616 [astro-ph.HE] .

[11] P. De la Torre Luque *et al.*, JCAP **2021**, 010 (2021).

[12] M. Aguilar *et al.* (AMS Collaboration), Phys. Rev. Lett. **120**, 021101 (2018).

[13] I. V. Moskalenko and S. G. Mashnik, in *ICRC*, ICRC, Vol. 4 (2003) p. 1969, arXiv:astro-ph/0306367 [astro-ph] .

[14] W. Webber, A. Soutoul, J. Kish, and J. Rockstroh, ApJ Supplement Series **144**, 153 (2003).

[15] R. Silberberg, C. Tsao, and A. Barghouty, ApJ **501**, 911 (1998).

[16] L. J. Gleeson and I. H. Urch, Astrophysics and Space Science **25**, 387 (1973).

[17] J.-M. Casandjian, Astrophys. J. **806**, 240 (2015), arXiv:1506.00047 [astro-ph.HE] .